Biochemical and Biophysical Research Communications 459 (2015) 553–559

Contents lists available at ScienceDirect

Biochemical and Biophysical Research Communications

journal homepage: www.elsevier.com/locate/ybbrc

Osteopontin-induced brown adipogenesis from white preadipocytes through a PI3K-AKT dependent signaling

Xiao-Juan Zhong [a, b, 1], Xiao-Dan Shen [a, b, 1], Jian-Bing Wen [a, b, 1], Ying Kong [a, b], Jia-Jia Chu [a, b], Guo-Qiang Yan [a, b], Teng Li [a, b], Dan Liu [a, b], Meng-Qing Wu [a, b], Guo-Hua Zeng [a, b], Ming He [a, b], Qi-Ren Huang [a, b, *]

[a] Jiangxi Provincial Key Laboratory of Basic Pharmacology, Nanchang University, Nanchang 330006, PR China
[b] Department of Pharmacology, School of Pharmaceutical Science, Nanchang University, Nanchang 330006, PR China

ARTICLE INFO

Article history:
Received 19 February 2015
Available online 6 March 2015

Keywords:
Osteopontin
Differentiation
Obesity
Adipocyte
PRDM16

ABSTRACT

Recent studies have shown that OPN (osteopontin) plays critical roles in cell survival, differentiation, bio-mineralization, cancer and cardiovascular remodeling. However, its roles in the differentiation of brown adipocytes and the underlying mechanisms remain unclear. Therefore, the aim of this study was to investigate the roles of OPN in the brown adipogenesis and the underlying mechanisms. It was shown that the OPN successfully induced the differentiation of 3T3-L1 white preadipocytes into the PRDM16$^+$ (PRD1-BF1-RIZ1 homologous domain containing 16) and UCP-1$^+$ (uncoupling protein-1) brown adipocytes in a concentration and time-dependent manner. Also, activation of PI3K (phosphatidylinositol 3-kinase)-AKT pathway was required for the OPN-induced brown adipogenesis. The findings suggest OPN plays an important role in promoting the differentiation of the brown adipocytes and might provide a potential novel therapeutic approach for the treatment of obesity and related disorders.

© 2015 Elsevier Inc. All rights reserved.

1. Introduction

Adipose tissue plays an important role in metabolic homeostasis, and consequently, change in its functions may lead to metabolic disorders, most notably type 2 diabetes mellitus (T2D), atherosclerosis (AS), hypertension, and cancers [1–3]. White adipocyte (WA) (predominantly existing in white adipose tissue) and brown adipocyte (BA) (predominantly in brown adipose tissue) differ in many aspects such as origin, distribution, morphology and functions [4,5]. The WA stores triglyceride (TG) and contributes to obesity, while the BA 'burns' fat through fatty acid-β-oxidation and contributes to weight loss [6,7]. Therefore, investigating the mechanisms underlying BA differentiation and brown adipogenesis would provide a novel strategy or avenue for prevention and treatment of obesity and related disorders.

Although WA and BA originate from the same mysenchymal stem cells, they differ in morphology and molecular phenotype [8,9]. Morphologically, mature BA is a multilocular cell abundant in lipid and mitochondrium, while mature WA is a unilocular cell deficient in the mitochondrium [10]. PRDM16 (PRD1-BF1-RIZ1 homologous domain containing 16) is recently identified as an early determinator of the brown adipogenesis, and UCP-1 (uncoupling protein-1) is generally considered as a BA specific protein marker [11,12]. Consequently, the BA is characterized as a PRDM16$^+$/UCP-1$^+$ adipocyte, and the WA as an angiotensin$^+$/resistin$^+$ cell. Therefore, these markers are commonly used to identify BA or WA [13,14]. Numerous studies have demonstrated that both cold exposure and lasting excitation of sympathetic nerves robustly promote brown adipose conversion from white preadipocytes, and this adaptive brown adipogenesis is beneficial to defend colds and bad states [15–17]. Given above, promotion of BA differentiation can be possibly used to fight against obesity. Unfortunately, transcriptional regulation mechanisms underlying the BA differentiation remain largely unclear.

Abbreviations: AS, atherosclerosis; BA, brown adipocyte; iOPN, intracellular OPN; OPN, osteopontin; PI3K, phosphatidylinositol 3-kinase; PRDM16, PRD1-BF1-RIZ1 homologous domain containing 16; UCP-1$^+$, uncoupling protein-1; SPP-1, secreted phosphoprotein-1; sOPN, secreted OPN; T2D, type 2 diabetes mellitus; TG, triglyceride; WA, white adipocyte.

* Corresponding author. Jiangxi Provincial Key Laboratory of Basic Pharmacology, Nanchang University, 461 Ba-Yi Street, Nanchang 330006, PR China. Fax: +86 791 86361839.
E-mail address: qrhuang@ncu.edu.cn (Q.-R. Huang).
[1] Equal contributions to this article.

http://dx.doi.org/10.1016/j.bbrc.2015.02.153
0006-291X/© 2015 Elsevier Inc. All rights reserved.

OPN (Osteopontin), known as SPP-1 (secreted phosphoprotein-1), are extensively expressed in diverse cells such as osteoblasts, endothelial cells, macrophages, T cells, hepatic stellate cells, and smooth muscle cells [18]. Recent studies have shown that OPN is implicated in many critical pathophysiological processes including bio-mineralization, differentiation, carcinogenesis and cardiovascular remodeling, etc [19,20]. However, its roles and the mechanisms underlying the differentiation of BA remain elusive. Therefore, the aim was to investigate the roles of OPN in brown adipogenesis and to explore the mechanisms underlying the differentiation.

2. Materials and methods

2.1. Materials

All chemicals were acquired commercially. High-glucose Dulbecco's modified Earle's medium (H-DMEM) was purchased from Gibco-BRL (NY, USA). Antibodies against OPN, PRDM16, UCP-1, AKT and β-actin (Santa Cruz Biotechnology, CA, USA), Phospho-AKT (serine473), and αvβ3 integrin (Cell Signaling Technology, MA, USA) were freshly prepared. OPN ELISA kit, KpnI and Xba were acquired from R&D Systems (MN, USA) and New England Biolabs (London, UK), respectively. Total RNA was isolated with QIAzol lysis reagent (Qiagen, Valencia, CA, USA). AKT inhibitor IV and LY294002 (Sigma–Aldrich, St. Louis, MO, USA) were dissolved in DMSO. All other chemicals were purchased from Sigma–Aldrich (St. Louis, MO, USA) unless otherwise specified.

2.2. DNA constructs and cell transfection

Flag-tagged OPN was amplified by PCR using full length OPN as a template, and sub-cloned into the pCMV5 vector as our previously described [21]. The sequences used here are as follows: sense (5′-GGGGTACCTATGAGATTGGCAGTGAT-3′) and antisense (5′-GCTCTAGACGCCTCTTCTTTAGTTGAC-3′). In addition, cell transfection was conducted following the manufacturer's instructions (Invitrogen). Briefly, 3T3-L1 cells were plated in the 6-well plate at 2–8 × 10^5 cells/well and were allowed to grow to 95% confluence. The cells were washed twice with the serum-free DMEM and transfected with 2 μg, 4 μg, 6 μg pCMV5-flag-OPN vector, respectively, and 4 μg pCMV5-flag empty vector was used as a control by Lipofectamine 2000 (Invitrogen). The cells were cultured at 37 °C in the 95% O_2–5% CO_2 humidified atmosphere. Six hours after transfection, the serum-free DMEM was replaced by the complete DMEM containing 10% FBS. Forty-eight hours after transfection, the cells were harvested and detected by Western blots.

2.3. Cell culture and differentiation

The 3T3-L1 white preadipocytes were obtained from the American Type Culture Collection (ATCC, USA). The 3T3-L1 cells were cultured as our previously described [22]. The method used for *In vitro* differentiation was adopted from the report by Tseng et al., 2008 [23]. Briefly, the 60% confluent 3T3-L1 white preadipocytes were incubated in the serum-free DMEM/F12 medium

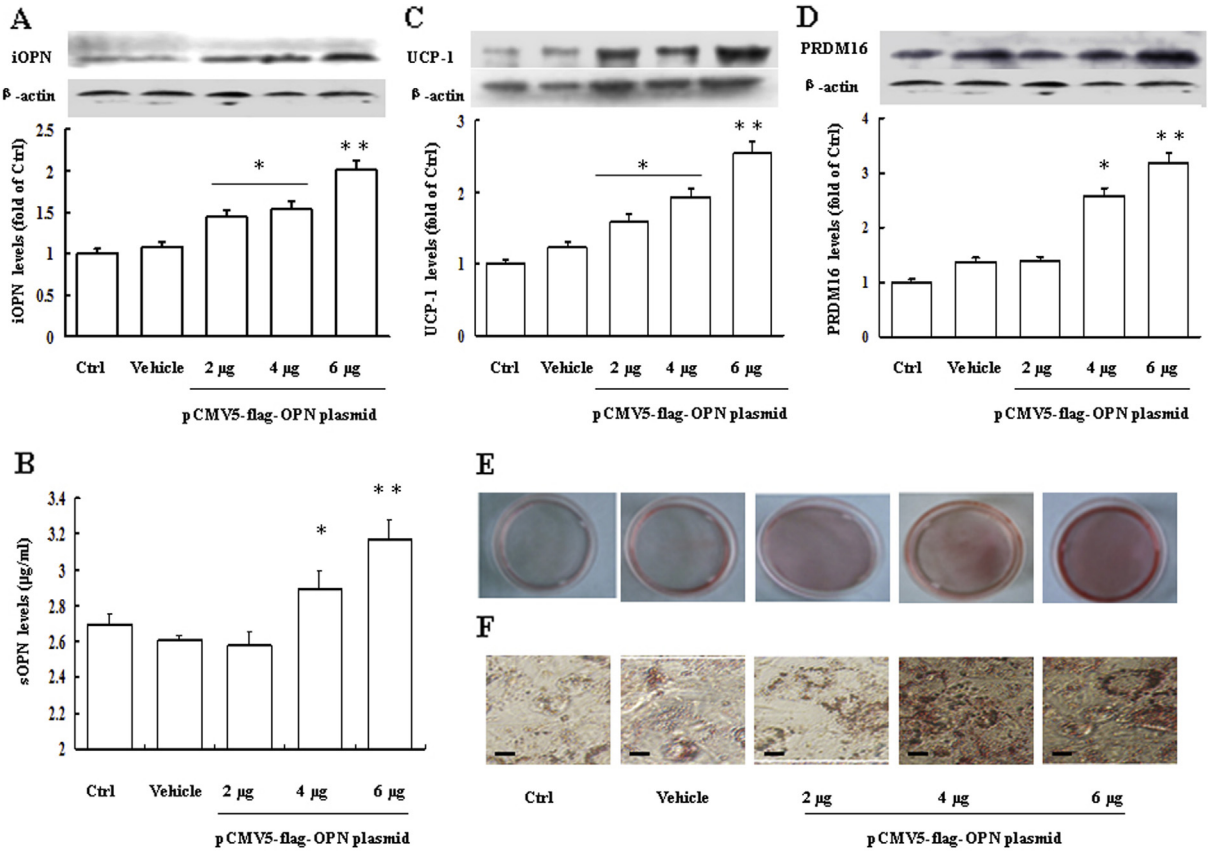

Fig. 1. Concentration-effect of OPN-induced brown adipogenesis. The expression of iOPN (A), UCP-1 (C), PRDM16 (D), and morphologic elements (oil-red O staining, E and F) of the transfected 3T3-L1 white preadipocytes with 2 μg, 4 μg, 6 μg pCMV5-flag-OPN vector, or 4 μg pCMV5-flag empty vector (Vehicle), and untransfected (Ctrl) 3T3-L1 white preadipocytes following differentiation for 6 days are shown. The sOPN (B) was measured from the supernatant following differentiation. Data are expressed as mean ± S.E.M. of 4 independent experiments. $^{*}P < 0.05$, $^{**}P < 0.01$, vs. Ctrl or Vehicle. Scale bars, 200 μm iOPN, intracellular OPN; sOPN, secreted OPN.

supplemented with the differentiation cocktail which contains 1 μM dexamethasone, 66 nM insulin, 15 mM HEPES, 1 nM T3, 33 μM biotin, 17 μM pantothenate, 10 μg/ml transferrin and 100 μg/ml penicillin-streptomycin in the absence or presence of 1 μg/ml rosiglitazone for 8 days. During the differentiation period, the medium was replaced with fresh one every 2 days.

2.4. Experimental protocols

2.4.1. Concentration-effect of OPN-induced brown adipogenesis

The 90% confluent 3T3-L1 white preadipocytes were transfected either with 2 μg, 4 μg, 6 μg pCMV5-flag-OPN vector or 4 μg pCMV5-flag empty vector (Vehicle), respectively. The untransfected 3T3-L1 cells were used as a control (Ctrl). Forty-eight hours after transfection, the transfection medium was substituted by the differentiation medium, and the cells were allowed to undergo differentiation for 6 days. At the end of differentiation, the cells were examined phenotypically and morphologically and an optimal OPN concentration for inducing differentiation was determined for further studies.

2.4.2. Time course of OPN-induced brown adipogenesis

The 90% confluent 3T3-L1 white preadipocytes were transfected with 6 μg pCMV5-flag-OPN vector. Forty-eight hours after transfection, the cells were allowed to undergo differentiation for 0, 2, 4, 6 and 8 days, respectively. The differentiated cells were examined phenotypically and morphologically and an optimal time for inducing differentiation by OPN was determined for further studies.

2.4.3. Effect of inhibition of αvβ3-PI3K-AKT pathway on the OPN-induced brown adipogenesis

The 90% confluent 3T3-L1 white preadipocytes were first transfected with 6 μg pCMV5-flag-OPN vector or 6 μg pCMV5-flag empty vector (as a control). Next, forty-eight hours after transfection, the 3T3-L1 cells were pretreated with 10 μM LY294002 (PI3K inhibitor, final concentration), 0.5 μM AKT IV(AKT inhibitor), and 5 μg/ml anti-αvβ3 integrin for 48 h, respectively. DMSO or 5 μg/ml IgG was used here as a vehicle, and negative control, respectively. Subsequently, the pretreated cells were allowed to undergo differentiation for 6 days. At the end, the cells were harvested and used for phenotypic and morphological examination.

2.5. Oil-red O staining

The differentiated 3T3-L1 cells were stained with oil-red O as previously described [24]. Briefly, the cells were washed twice with phosphate-buffered saline (PBS), and then fixed with 10% paraformaldehyde at room temperature for 10 min, then the fix solution was removed and the cells were again washed twice with the PBS. Fresh oil-red O solution (0.5% oil-red O in isopropyl alcohol) was added and incubated at room temperature for 1 h. Next, the staining solution was removed and the cells were washed with the PBS for 3 times. Finally, the stained cells were microscopically examined.

2.6. Western blot assay

Western blot assay was performed by a modification of traditional technique as our previously described [25]. Briefly, the

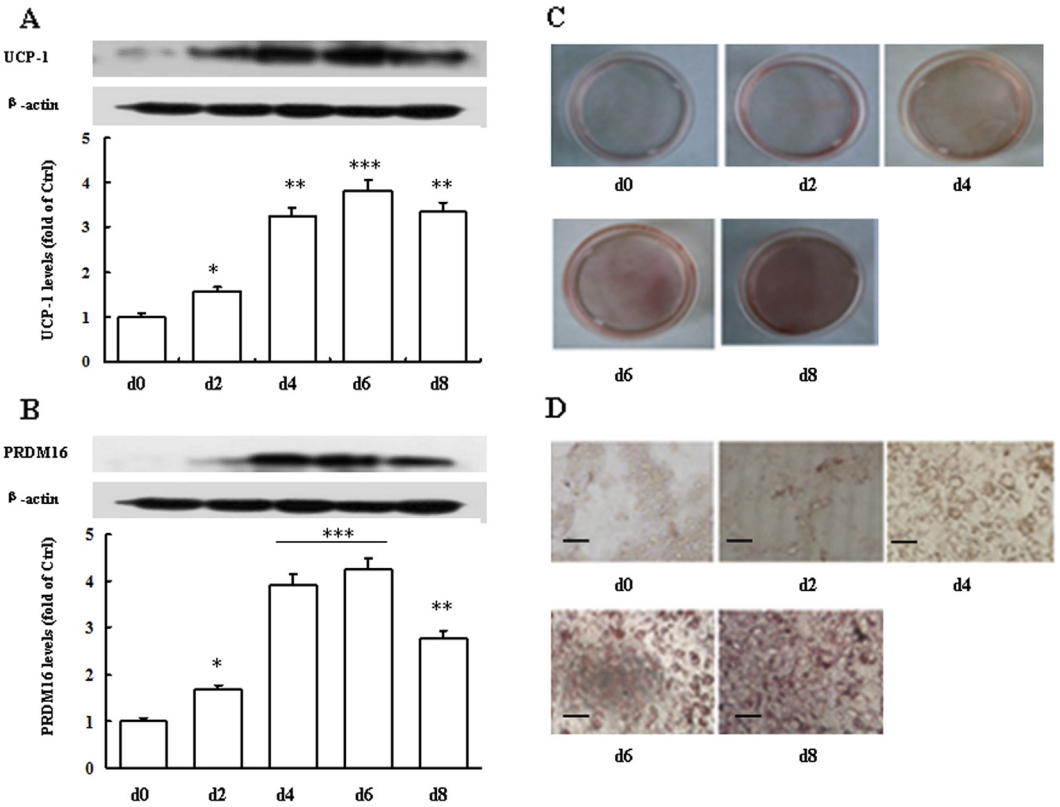

Fig. 2. Time course of OPN-induced brown adipogenesis. The expression of UCP-1 (A), PRDM16 (B), and morphologic elements (oil-red O staining, C and D) of the transfected 90% confluent 3T3-L1 white preadipocytes with 6 μg pCMV5-flag-OPN vector following differentiation for 0, 2, 4, 6 and 8 days are shown. Data are expressed as mean ± S.E.M. of 4 independent experiments. $^{*}P < 0.05$, $^{**}P < 0.01$, $^{***}P < 0.001$ vs. day 0. Scale bars, 200 μm.

differentiated cells were harvested and lysed in the lysis buffer (25 mM Tris–HCl, *p*H 7.8, 100 mM NaCl, 1 mM EDTA, 1 mM EGTA, 1 mM Na_3VO_4, and 25 mM glycerol phosphate, 1 mM dithiothreitol, 1% Nonidet P-40 (w/v), 10 μg/ml leupeptin and 10 μg/ml aprotinin). The lysates were centrifuged at 12,000 × g at 4 °C for 15 min, and the protein concentration was determined using Bio-Rad Protein Assay kit (Bio-Rad Laboratories, CA, USA). Fifty micrograms of total proteins were separated by 8% SDS-PAGE. Bands on the gels were blotted onto polyvinylidene fluoride membranes (Bio-Rad Laboratories, CA, USA) and then the membranes were incubated with antibodies against various proteins at a 1:1000 dilution. A horseradish peroxidase-conjugate anti-rabbit antibody (Amersham Pharmacia Biotech) was used as a secondary antibody at a 1:2000 dilution. Immunoreactive bands were visualized by the enhanced chemiluminescence (ECL) detection system (Perkin Elmer Life Science Inc., MA, USA).

2.7. Quantitative assay of sOPN by ELISA

The levels of sOPN (secreted OPN) were checked using the Quantikine ELISA Kits following the manufacturer's instruction (R&D Systems, MN, USA). Fifty microliters of cell supernatants were added to a 96-well polystyrene microplate precoated with OPN monoclonal antibody and incubated for 2 h at room temperature on the shaker. After gentle washes with PBS 5 times, 100 μl secondary antibody conjugated to horseradish peroxidase was added and incubated for 2 h at room temperature, followed by an addition of 100 μl substrate solution and incubation for 30 min at room temperature. Ultimately, 100 μl stop solution was added and the optical density (OD) was determined at 450 nm in a microplate reader (Bio-Rad Laboratories, CA, USA).

2.8. Statistical analysis

All data were expressed as the means ± S.E.M. Significance was tested with unpaired t test, one-way ANOVA and homogeneity test of variance. A P value <0.05 was considered to be statistically significant.

3. Results and discussion

BA is specialized to dissipate chemical energy in the form of heat, as a physiological defense against cold and obesity [6,7]. Understanding the mechanisms underlying the brown adipogenesis would help to develop the drugs that promote BA conversion from white preadipocytes and may lead to new avenues for prevention and treatment of metabolic diseases such as obesity and T2D. A large number of scientists worldwide have been making many beneficial attempts at this field [26–28]. Unfortunately, knowledge in this field is relatively lacking, and especially the mechanisms underlying BA conversion from white preadipocytes

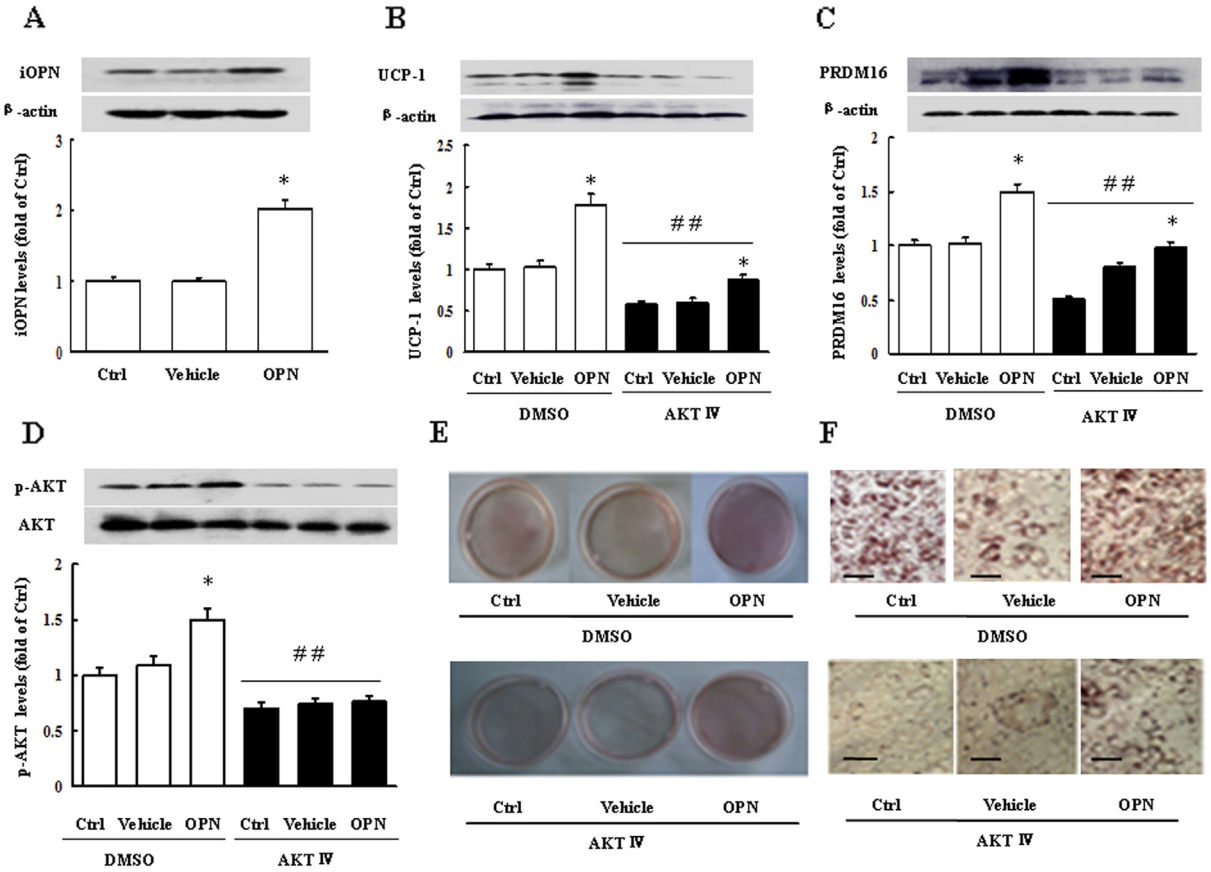

Fig. 3. Phosphorylation of AKT is required for OPN-induced brown adipogenesis. The expression of iOPN (A) and the effects of AKT Ⅳ(AKT inhibitor, 0.5 μM), or DMSO (as a vehicle control) on the expression of UCP-1 (B), PRDM16 (C), phosphorylated AKT(D) and morphologic elements (oil-red O staining, E and F) of the transfected 90% confluent 3T3-L1 white preadipocytes with 6 μg pCMV5-flag-OPN vector, or 6 μg pCMV5-flag empty vector (Vehicle), and untransfected (Ctrl) 3T3-L1 white preadipocytes following differentiation for 6 days are shown. The OPN-induced brown adipogenesis was inhibited by AKT Ⅳ (AKT inhibitor). Data are expressed as mean ± S.E.M. of 4 independent experiments. $^{*}P < 0.05$, vs. Ctrl or Vehicle. $^{\#\#}P < 0.01$, vs. DMSO. Scale bars, 200 μm.

still remains enigmatic. This necessitates the investigation of brown adipogenesis and the underlying molecular mechanisms.

OPN is a secreted glycoprotein that functions as a ligand to αvβ3 integrin and possibly other receptors. It is expressed in a wide range of cells and tissues including osteoblasts, odontoblasts, various tumor cell lines, extraosseous cells in the inner ear, as well as brain, kidney, and placenta [29,30]. Recent studies have shown that OPN plays critical roles not only in cell survival, adhesion, migration, differentiation and bio-mineralization as well as cancer and cardiovascular remodeling [31]. However, its roles in differentiation of brown adipocytes and the underlying mechanisms remain unclear. Therefore, the role of the OPN in brown adipogenesis was explored. Hence, an engineered vector carrying different amount (2, 4, or 6 μg) of Opn cDNA (Opn-containing vector) was transfected to an immortalized 3T3-L1 white preadipocytes deficient in OPN to examine its effect on brown adipogenesis. As expected, 2 days after transfection, both iOPN (intracellular OPN) and sOPN (secreted OPN) levels in the transfected vector with Opn cDNA were strikingly higher than those in the control (Ctrl) or empty vector (Vehicle), indicating that the vector transduction was successful (Fig. 1A, B). The results of further BA differentiation experiments also showed that the levels of the BA-specific phenotypic markers such as UCP-1 and PRDM16 were remarkably elevated after the differentiation for 6 days with the increase in transfection amount of the Opn-containing vector, and the increased levels in the 6 μg Opn-containing vector group were the most significant (Fig. 1C, D). Thus, 6 μg Opn-containing vectors were regarded as the optimal transfection concentration and were therefore used in subsequent experiments. Similarly, the morphological results from oil-red O staining also vividly displayed that with the increase of transfected-OPN cxoncentration, the cell appearance changed from unilocular and less lipid-accumulating to a multilocular and richer lipid-containing (Fig. 1E, F). Together, these data indicated that the OPN-driven BA adipogenesis was concentration-dependent.

Next, we investigated time course of the OPN-induced BA conversion from 3T3-L1 cells. As shown in Fig. 2, the levels of the BA-specific markers gradually increased with the elongation of the OPN-induction time, peaked at day 6 and then declined at day 8 of induction (Fig. 2A, B). Similarly, the number of BA also gradually increased and peaked at day 6 of induction (Fig. 2C, D). Therefore, 6 days was chosen as the induction time for the subsequent experiments.

Next, the molecular mechanisms for OPN-driven BA adipogenesis from white preadipocytes were investigated. Previous studies have indicated that PI3K-AKT signaling is involved in cell proliferation, differentiation and apoptosis [32,33]. AKT is a kinase and phosphorylation of AKT at serine 473 is critical for the activation of AKT. Whether the OPN-induced brown adipogenesis is also mediated by phosphorylation of AKT at serine 473 was tested. AKT IV (a specific AKT inhibitor) was used to inhibit the phosphorylation of the kinase. As shown in Fig. 3, OPN-induction regimen (6 μg and 6 days) increased the levels of iOPN considerably (Fig. 3A).

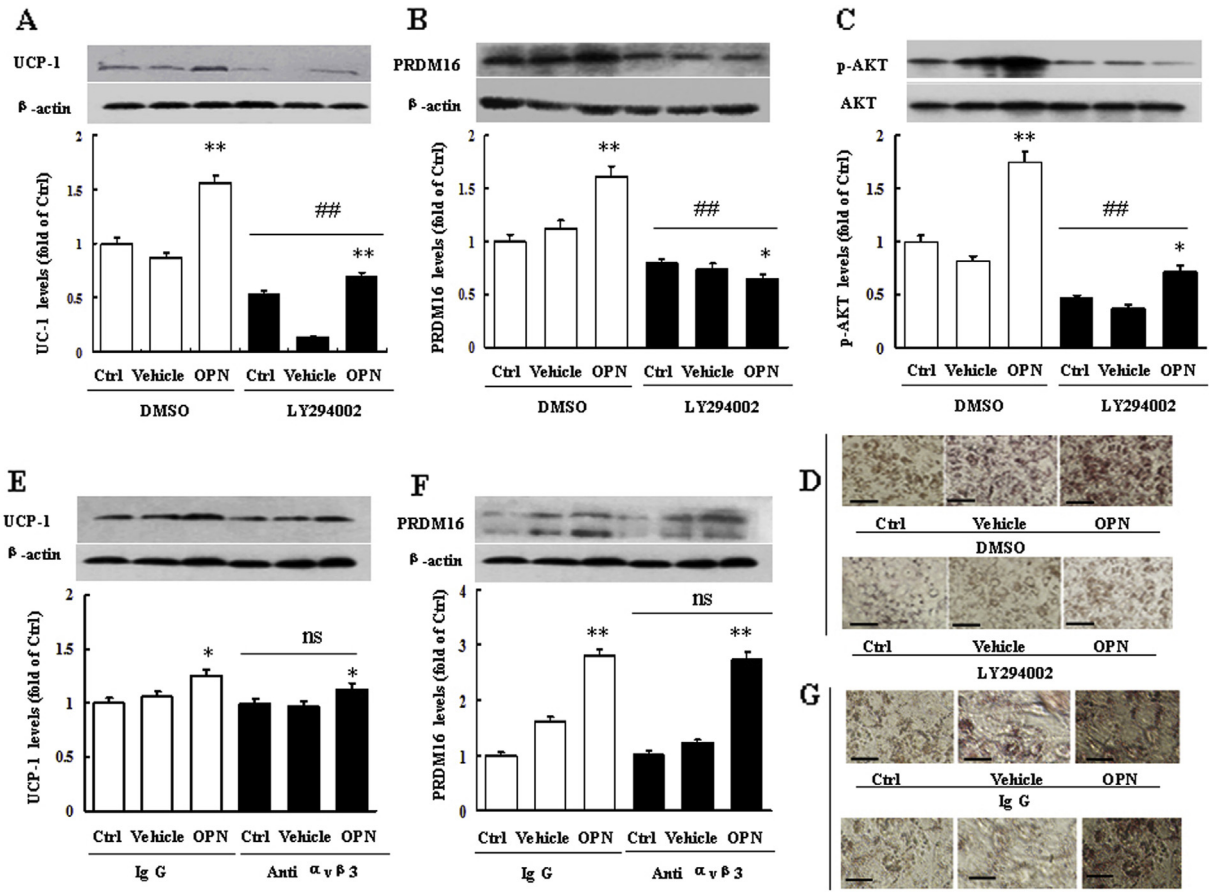

Fig. 4. OPN-induced brown adipogenesis is via a PI3K-AKT but not avβ3 integrin dependent pathway. The effects of LY294002 (PI3K inhibitor, 10 μM), anti-αvβ3 integrin (5 μg/ml), or DMSO (as a vehicle control) on the expression of UCP-1 (A, E), PRDM16 (B, F), phosphorylated AKT(C), and morphologic elements (D and G) of the transfected 90% confluent 3T3-L1 white preadipocytes with 6 μg pCMV5-flag-OPN vector, or 6 μg pCMV5-flag empty vector (Vehicle), and untransfected (Ctrl) 3T3-L1 white preadipocytes following differentiation for 6 days are shown. The OPN-induced brown adipogenesis was inhibited by LY294002 (PI3K inhibitor), not by anti-αvβ3 integrin (avβ3 integrin antibody).Data are expressed as mean ± S.E.M. of 4 independent experiments. $^{*}P < 0.05$, $^{**}P < 0.01$, vs. Ctrl or Vehicle. $^{\#\#}P < 0.01$, vs. DMSO. ns, no significance. Scale bars, 200 μm.

Simultaneously, it dramatically elevated the expression of the BA-specific makers (Fig. 3B, C). Moreover, it also significantly boosted the phosphorylation of AKT (Fig. 3D).

Another question is whether the relationship between the expression induction of the markers and the phosphorylation of AKT elicited by OPNA was accompanying or causal. To address this question, AKT IV, an inhibitor of AKT, was used to suppress the phosphorylation of AKT. Indeed, treatment with AKT IV markedly reduced the phosphorylation of AKT compared with the vehicle (DMSO) treated cells (Fig. 3D). Moreover, AKT IV notably counteracted the OPN-mediated effect on the expression of PRDM16 and UCP-1, suggesting that the phosphorylation of AKT is indispensible for the OPN-induced expression of BA specific markers in 3T3-L1 white preadipocytes (Fig. 3B, C). Similarly, oil-red O staining showed that OPN markedly induced lipid accumulation and AKT IV reversed the effects of OPN (Fig. 3E, F). Taken together, these data uniformly demonstrated that the phosphorylation of AKT was required for the OPN-induced brown adipogenesis from white preadipocytes.

As a critical intracellular messenger involved in cell differentiation, AKT activity can be regulated by many bio-substances such as PI3K (phosphatidylinositol 3-kinase). OPN binds to integrins or CD44 through which it can signal to downstream targets including PI3K [34]. It would be interesting to know whether PI3K is involved in the OPN-induced brown adipogenesis and whether the effects of PI3K are through the regulation of the activity of AKT. Treatment of 3T3-L1 cells for 2 days with 10 μM LY294002, a pharmacological inhibitor of PI3K, dramatically counteracted the increase in the phosphorylation of AKT induced by OPN compared with the DMSO-treated cells, suggesting that PI3K indeed is an upstream kinase of AKT. Moreover, treatment with LY294002 also offset the increase of expression of specific markers on BA and lipid accumulation induced by OPN, strongly suggesting that activation of PI3K is necessary for the OPN-induced brown adipogenesis and is an upstream event for AKT phospharylation (Fig. 4A–D).

Cellular responses to OPN have been shown to be mediated by its receptors [35] and OPN has been demonstrated to function as a ligand to αvβ3 integrin and possible other receptors such as CD44, etc. [36]. It is possible that OPN-induced brown adipogenesis is mediated by a cascade of reactions involving αvβ3 integrin or other receptors first and then PI3K-AKT pathway, which lead to expression of PRDM16 and UCP-1. To test the possible role of αvβ3 integrin in the OPN-induced brown adipogenesis, the antibody anti-αvβ3 was used to neutralize αvβ3 integrin and unrelated immunoglobulin G (IgG) was used as a control. The treatment of 3T3-L1 cells with anti-αvβ3 did not appear to block the effects of OPN on 3T3-L1 cell differentiation, indicating that the neutralization of αvβ3 integrin did not alter the OPN-mediated expression of the BA markers and lipid accumulation (Fig. 4 E–G). These data also suggest that the role of OPN-induced brown adipogenesis is αvβ3 integrin-independent, implying other receptors such as $\alpha_v\beta5$, $\alpha_v\beta6$ or CD44 are likely to involve in the OPN-induced brown adipogenesis. Further studies are needed to confirm this notion.

In summary, the present study for the first time showed that OPN could induce brown adipogenesis from white preadipocytes in a PI3K-AKT signaling-dependent and αvβ3 integrin-independent fashion. The study might provide a potential novel therapeutic approach for the treatment of obesity and related disorders with OPN or its analogs, which could induce an increase in brown adipocytes through adipogenesis and lead to increase in energy expenditure.

Conflict of interest

None.

Acknowledgments

This study was supported by the research grants from the Natural Scientific Foundation of China (81360060, 81070633, 30860111, and 30660058) and the research projects from the Ministry of Science & Technology, Jiangxi, China (20123BCB22005).

Transparency document

Transparency document related to this article can be found online at http://dx.doi.org/10.1016/j.bbrc.2015.02.153.

References

[1] P. Seale, S. Kajimura, B.M. Spiegelman, Transcriptional control of brown adipocyte development and physiological function-of mice and men, Genes Dev. 23 (2009) 788–797.
[2] B. Cannon, J. Nedergaard, Brown adipose tissue: function and physiological significance, Physiol. Rev. 84 (2004) 277–359.
[3] J. Ishibashi, P. Seale, Beige can be slimming, Science 328 (2010) 1113–1114.
[4] P. Seale, H.M. Conroe, J. Estall, S. Kajimura, A. Frontini, J. Ishibashi, P. Cohen, S. Cinti, B.M. Spiegelman, PPRDM16 determines the thermogenic program of subcutaneous white adipose tissue in mice, J. Clin. Invest. 121 (2011) 96–105.
[5] S. Kajimura, P. Seale, K. Kubota, E. Lunsford, J.V. Frangioni, S.P. Gygi, B.M. Spiegelman, Initiation of myoblast/brown fat switch through a PRDM16-C/EBP-β transcriptional complex, Nature 460 (2009) 1154–1158.
[6] P. Seale, M.A. Lazar, Brown fat in humans: turning up the heat on obesity, Diabetes 58 (2009) 1482–1484.
[7] S.R. Farmer, Molecular determinants of brown adipocyte formation and function, Genes Dev. 22 (2008) 1269–1275.
[8] S. Enerback, The origins of brown adipose tissue, N. Engl. J. Med. 360 (2009) 2021–2023.
[9] P. Seale, B. Bjork, W. Yang, S. Kajimura, S. Kuang, A. Scime, S. Devarakonda, S. Chin, H.M. Conroe, E.B. Hediye, P. Tempst, M.A. Rudnicki, D.R. Beier, B.M. Spiegelman, PRDM16 controls a brown fat/skeletal muscle switch, Nature 454 (2008) 961–967.
[10] T. Zhang, H. Guan, K. Yang, Keratinocyte growth factor promotes preadipocyte proliferation via an autocrine mechanism, J. Cell. Biochem. 109 (2010) 737–746.
[11] P. Seale, S. Kajimura, W. Yang, S. Chin, L. Rohas, M. Uldry, G. Tavernier, D. Langin, B.M. Spiegelman, Transcriptional control of brown fat determination by PRDM16, Cell Metab. 6 (2007) 38–54.
[12] S. Kajimura, P. Seale, T. Tomaru, E.B. Hediye, M.P. Cooper, J.L. Ruas, S. Chin, P. Tempst, M.A. Lazar, B.M. Spiegelman, Regulation of the brown and white fat gene programs through a PRDM16/CtBP transcriptional complex, Genes Dev. 22 (2008) 1397–1409.
[13] B. Xue, A. Coulter, J.S. Rim, R.A. Koza, L.P. Kozak, Transcriptional synergy and the regulation of Ucp1 during brown adipocyte induction in white fat depots, Mol. Cell. Biol. 25 (2005) 8311–8322.
[14] R.K. Gupta, Z.N. Arany, P. Seale, R.J. Mepani, L. Ye, H.M. Conroe, Y.A. Roby, H. Kulaga, R.R. Reed, B.M. Spiegelman, Transcriptional control of preadipocyte determination by Zfp423, Nature 464 (2010) 619–623.
[15] G. Barbatelli, I. Murano, L. Madsen, Q. Hao, M. Jimenez, K. Kristiansen, J.P. Giacobino, R. De Matteis, S. Cinti, The emergence of cold-induced brown adipocytes in mouse white fat depots is predominantly determined by white to brown adipocyte transdifferentiation, Am. J. Physiol. Endocrinol. Metab. 298 (2010) E1244–E1253.
[16] M. Klingenspor, Cold-induced recruitment of brown adipose tissue thermogenesis, Exp. Physiol. 88 (2003) 141–148.
[17] M.O. Ribeiro, S.D. Carvalho, J.J. Schultz, G.T.S. Chiellini, A. Scanlan, C. Bianco, G.A. Brent, Thyroid hormone-sympathetic interaction and adaptive thermogenesis are thyroid hormone receptor isoform-specific, J. Clin. Invest. 108 (2001) 97–105.
[18] S.A. Lund, C.M. Giachelli, M. Scatena, The role of osteopontin in inflammatory processes, J. Cell Commun. Signal. 3 (2009) 311–322.
[19] F.W. Kiefer, M. Zeyda, K. Gollinger, B. Pfau, A. Neuhofer, T. Weichhart, M.D. Saemann, R. Geyeregger, M. Schlederer, L. Kenner, T.M. Stulnig, Neutralization of osteopontin inhibits obesity-induced inflammation and insulin resistance, Diabetes 59 (2010) 935–946.
[20] M. Singh, C.R. Foster, S. Dalal, K. Singh, Osteopontin: role in extracellular matrix deposition and myocardial remodeling post-MI, J. Mol. Cell. Cardiol. 48 (2010) 538–543.
[21] M. Zang, J. Gong, L. Luo, J. Zhou, X. Xiang, W. Huang, Q.R. Huang, X. Luo, M. Olbrot, Y. Peng, C. Chen, Z. Luo, Characterization of Ser338 phosphorylation for Raf-1 activation, J. Biol. Chem. 283 (2008) 31429–31437.
[22] Q.R. Huang, Q. Li, Y.H. Chen, L. Li, L.L. Liu, S.H. Lei, H.P. Chen, W.J. Peng, M. He, Involvement of anion exchanger-2 in apoptosis of endothelial cells induced by high glucose through an mPTP-ROS-Caspase-3 dependent pathway, Apoptosis 15 (2010) 693–704.

[23] Y.H. Tseng, E. Kokkotou, T.J. Schulz, T.L. Huang, J.N. Winnay, C.M. Taniguchi, T.T. Tran, R. Suzuki, D.O. Espinoza, Y. Yamamoto, M.J. Ahrens, A.T. Dudley, A.W. Norris, R.N. Kulkarni, C.R. Kahn, New role of bone morphogenetic protein 7 in brown adipogenesis and energy expenditure, Nature 454 (2008) 1000–1004.
[24] L. Sun, H. Xie, M.A. Mori, R. Alexander, B. Yuan, S.M. Hattangadi, Q. Liu, C.R. Kahn, H.F. Lodish, MiR-193b-365, a brown fat enriched microRNA cluster, is essential for brown fat differentiation, Nat. Cell Biol. 13 (2011) 958–965.
[25] L.L. Liu, L. Yan, Y.H. Chen, G.H. Zeng, Y. Zhou, H.P. Chen, W.J. Peng, M. He, Q.R. Huang, A role for diallyl trisulfide in mitochondrial antioxidative stress contributes to its protective effects against vascular endothelial impairment, Eur. J. Pharmacol. 725 (2014) 23–31.
[26] A.G. Elefanty, E.G. Stanley, Efficient generation of adipocytes in a dish, Nat. Cell Biol. 14 (2012) 126–127.
[27] E. Ravussin, C. Bouchard, Human genomics and obesity: finding appropriate drug targets, Eur. J. Pharmacol. 410 (2000) 131–145.
[28] Y. Chang, Z.G. She, K. Sakimura, A. Roberts, K. Kucharova, D.H. Rowitch, W.B. Stallcup, Ablation of NG2 proteoglycan leads to deficits in brown fat function and to adult onset obesity, PLoS One 7 (2012) e30637.
[29] L.F. Brown, B. Berse, L. Vande Water, A. Papadopoulos-Sergiou, C.A. Perruzzi, E.J. Manseau, H.F. Dvorak, D.R. Senger, Expression and distribution of osteopontin in human tissues: widespread association with luminal epithelial surfaces, Mol. Biol. Cell 3 (1992) 1169–1180.
[30] P.H. Anborgh, J.C. Mutrie, A.B. Tuck, A.F. Chambers, Pre- and post-translational regulation of osteopontin in cancer, J. Cell Commun. Signal. 5 (2011) 111–122.
[31] J.S. Shao, S.L. Cheng, J. Sadhu, D.A. Towler, Inflammation and the osteogenic regulation of vascular calcification: a review & perspective, Hypertension 55 (2010) 579–592.
[32] S.P. Kim, J.M. Ha, S.J. Yun, E.K. Kim, S.W. Chung, K.W. Hong, C.D. Kim, S.S. Bae, Transcriptional activation of peroxisome proliferator-activated receptor-gamma requires activation of both protein kinase A and Akt during adipocyte differentiation, Biochem. Biophys. Res. Commun. 399 (2010) 55–59.
[33] B.W. Robertson, M.A. Chellaiah, Osteopontin induces β-catenin signaling through activation of Akt in prostate cancer cells, Exp. Cell Res. 316 (2010) 1–11.
[34] J. Chapman, P.D. Miles, J.M. Ofrecio, J.G. Neels, J.G. Yu, J.L. Resnik, J. Wilkes, S. Talukdar, D. Thapar, K. Johnson, D.D. Sears, Osteopontin is required for the early onset of high fat diet-induced insulin resistance in mice, PLoS One 5 (2010) e13959.
[35] J. Dai, Z. Cao, Y. Kang, K. Fan, G. Ji, H. Yang, H. Wang, J. Gao, H. Wang, Y. Guo, A functional motif QLYxxYP is essential for osteopontin induced T lymphocyte activation and migration, Biochem. Biophys. Res. Commun. 380 (2009) 715–720.
[36] B. Christensen, E. Kläning, M.S. Nielsen, M.H. Andersen, E.S. Sørensen, C-terminal modification of osteopontin inhibits interaction with the αVβ3-integrin, J. Biol. Chem. 287 (2012) 3788–3797.